Dissociation of amyloid fibrils of α-synuclein and transthyretin by pressure reveals their reversible nature and the formation of water-excluded cavities

Débora Foguel[†‡], Marisa C. Suarez[†], Astria D. Ferrão-Gonzales[†], Thais C. R. Porto[†], Leonardo Palmieri[†], Carla M. Einsiedler[†], Leonardo R. Andrade[§], Hilal A. Lashuel[¶], Peter T. Lansbury[¶], Jeffery W. Kelly[‖], and Jerson L. Silva[†]

[†]Departamento de Bioquímica Médica, Instituto de Ciências Biomédicas, Universidade Federal do Rio de Janeiro, Rio de Janeiro, 21941-590, Brazil; [§]Laboratório de Biomineralização, Instituto de Ciências Biomédicas, Universidade Federal do Rio de Janeiro, Cidade Universitária, Rio de Janeiro, 21941-590, Brazil; [¶]Center for Neurologic Diseases, Brigham and Women's Hospital, and Department of Neurology, Harvard Medical School, Boston, MA 02115; and [‖]The Scripps Research Institute, 10550 North Torrey Pines Road, MB 12, La Jolla, CA 92037

Communicated by Jiri Jonas, University of Illinois at Urbana–Champaign, Urbana, IL, June 27, 2003 (received for review April 14, 2003)

Protein misfolding and aggregation have been linked to several human diseases, including Alzheimer's disease, Parkinson's disease, and systemic amyloidosis, by mechanisms that are not yet completely understood. The hallmark of most of these diseases is the formation of highly ordered and β-sheet-rich aggregates referred to as amyloid fibrils. Fibril formation by WT transthyretin (TTR) or TTR variants has been linked to the etiology of systemic amyloidosis and familial amyloid polyneuropathy, respectively. Similarly, amyloid fibril formation by α-synuclein (α-syn) has been linked to neurodegeneration in Parkinson's disease, a movement disorder characterized by selective degeneration of dopaminergic neurons in the substantia nigra. Here we show that consecutive cycles of compression–decompression under aggregating conditions lead to reversible dissociation of TTR and α-syn fibrils. The high sensitivity of amyloid fibrils toward high hydrostatic pressure (HHP) indicates the existence of packing defects in the fibril core. In addition, through the use of HHP we are able to detect differences in stability between fibrils formed from WT TTR and the familial amyloidotic polyneuropathy-associated variant V30M. The fibrils formed by WT α-syn were less susceptible to pressure denaturation than the Parkinson's disease-linked variants, A30P and A53T. This finding implies that fibrils of α-syn formed from the variants would be more easily dissolved into small oligomers by the cellular machinery. This result has physiological importance in light of the current view that the pathogenic species are the small aggregates rather the mature fibrils. Finally, the HHP-induced formation of fibrils from TTR is relatively fast (≈60 min), a quality that allows screening of antiamyloidogenic drugs.

In the last decade, effective treatments for several amyloidogenic and misfolding diseases have been sought (1, 2). In all of these diseases, the protein associated undergoes a conformational change and self-assembly to form highly ordered and β-sheet-rich structures referred to as amyloid fibrils. The process of amyloid fibril formation has been linked to tissues or organ dysfunction: heart and peripheral nerves in the case of transthyretin (TTR), and neurodegeneration in the case of amyloid-β peptide (Alzheimer's disease) and α-synuclein (α-syn) (Parkinson's disease) (3–6).

Parkinson's disease is the second most common neurodegenerative disorder in humans. It is associated with resting tremor, postural rigidity, and progressive degeneration of dopaminergic neurons in the substantia nigra pars compacta (6). Characteristic pathological features of Parkinson's disease include Lewy bodies, which are juxtanuclear-ubiquitinated proteinaceous inclusions in neuronal perikarya, and Lewy neurites, which are similar protein aggregates found in neuronal processes (7). Biochemical analysis of these inclusions revealed that α-syn is the major constituent of these neuronal inclusions, which points to its role in the ethiology of this disease (8). Moreover, two missense mutations in the gene encoding α-syn are linked to dominantly inherited Parkinson's disease, thereby directly implicating α-syn in the disease pathogenesis (9).

Amyloid fibril formation by WT TTR is responsible for senile systemic amyloidosis, a disease that affects 25% of people >80 years old, and is characterized by heavy amyloid deposits in the heart (3). More than 80 point mutants of TTR have been described thus far, most of them involved in familial amyloidotic polyneuropathy (FAP) (10). In general, FAP patients present the first symptoms by the second or third decade with peripheral neuropathy, cardiomyopathy, carpal tunnel syndrome, and vitreous opacities (3). The most widespread variant of TTR contains the substitution V30M in β-strand B, one of the eight β-strands present in TTR (5).

Here we describe the reversible dissociation of fibrils of α-syn and TTR assisted by high hydrostatic pressure (HHP). Pressure can change the balance between misfolding and folding in different ways, as recently demonstrated in rhodanese (11), the tailspike protein of bacteriophage P22 (12), myoglobin (13), and the amyloidogenic protein TTR (14). Pressure is well known to disrupt hydrophobic interactions and eliminate water-excluded cavities (15). We show that the interactions underlying aggregation *in vitro* can be reversed. Interestingly, the time and amount of pressure needed to dissociate the fibrils do not differ significantly from (or are even less than) those required to dissociate native oligomeric proteins. Through the use of HHP we can detect differences in stability between α-syn fibrils composed by the variant A30P, A53T, and WT protein. In addition, in view of the rapidity with which fibrils of α-syn and TTR undergo disassembly upon compression and aggregation after decompression (TTR), we propose the use of this methodology for drug screening.

BIOPHYSICS

Methods

TTR Fibril Formation and Dissociation. Recombinant TTR was expressed and purified as described (16). Soluble WT or V30M TTR (3.5 or 1 μM of tetramers, respectively) was compressed at 3,000 bar (1 bar = 100 kPa) during 30 min at 37°C at pH 5. After this time, pressure was released, and the light scattering was recorded with time as a measurement of aggregation, exciting the samples at 320 nm and collecting the light at 90° through the monochromator (315–325 nm). Light scattering and fluorescence were measured in an ISS spectrofluorimeter (Champaign, IL). All TTR experiments were performed in 50 mM Mes containing 100 mM KCl at pH 5.0.

Bis-(8-Anilinonaphthalene-1-sulfonate) (bis-ANS) Binding. The bis-ANS binding was evaluated from its fluorescence on exciting the sample at 360 nm and collecting the emission in the range between 300 and 600 nm.

Abbreviations: TTR, transthyretin; α-syn, α-synuclein; Trp, tryptophan; TEM, transmission electron microscopy; bis-ANS, bis-(8-anilinonaphthalene-1-sulfonate); FAP, familial amyloidotic polyneuropathy; HHP, high hydrostatic pressure.

[‡]To whom correspondence should be addressed. E-mail: foguel@bioqmed.ufrj.br.

α-Syn Fibril Formation and Dissociation. Recombinant α-syn was expressed and purified as described (17). Fibrils of α-syn were obtained by incubating 140 μM of each sample (WT, A30P, and A53T) at atmospheric pressure and 37°C, under gentle agitation. The experiments were performed in 5 mM Tris·HCl, 100 mM NaCl, and 0.02% NaN_3 at pH 7.5.

CD. CD spectra were recorded in a Jasco-715 spectropolarimeter (Jasco, Tokyo). The baselines (buffer alone) were subtracted.

Congo Red and Thioflavin T Binding. Proteins were diluted to a final concentration of 10 μM in buffer (10 mM sodium phosphate/2.7 mM KCl/137 mM NaCl, pH 7.4) containing 2.5 μM Congo red. A_{477} and A_{540} were recorded and used to calculate the number of moles of Congo red bound per liter, according to Glover *et al.* (18). Thioflavin T binding was evaluated from the increase in spectral area obtained on exciting the sample at 446 nm and collecting the emission in the range 460–560 nm. The experiments were performed in 50 mM glycine-NaOH at pH 8.5.

Transmission Electron Microscopy (TEM). The ultrastructure of α-syn fibrils was observed by TEM by using negative staining. The fibril solution (0.5 mg/ml) was diluted 20-fold in water and then 10 μl of this solution was deposited on a Formvar-coated copper grid. The grids were blotted to remove excess material, fixed with 10 μl uranyl acetate (2% aqueous solution) for 1 min, and examined in a JEOL 1200EX, operated at 80 kV.

Results

Pressure-Induced Dissociation of Preformed Fibrils of TTR. Previous *in vitro* studies have shown that TTR amyloid fibril formation requires tetramer dissociation to an alternatively folded monomer, which then self-assembles into a ladder of soluble oligomeric intermediates, ultimately affording amyloid fibrils (19–23). We have recently shown that after decompression, WT TTR forms fibrils under mild conditions (pH 5–5.6, 37°C, [TTR] ≥ 1 μM) (14). Using size-exclusion chromatography and bis-ANS binding, we demonstrated that the main species recovered after decompression under nonaggregating conditions (1°C) is a tetramer with an altered conformation (T_4*) and with weaker association between the subunits. This species is highly amyloidogenic, because under appropriate conditions (pH 5–5.6, 37°C) it aggregates after pressure release, whereas lower pHs (pH 4–4.4) are usually required to induce the aggregation of the native WT TTR tetramer.

To determine whether amyloid fibrils were susceptible to HHP, fibrils of WT TTR and the FAP-associated variant V30M were produced and subjected to high pressure (Fig. 1). Initial fibrils were produced by subjecting soluble, tetrameric WT or V30M TTR to high pressure for 30 min at pH 5.0 (37°C) (Fig. 1*A*), which has been shown to lead to the population of the amyloidogenic form of TTR (14). The pressure was then released (Fig. 1*B*), and light scattering was used to monitor TTR fibril formation, as described (14). V30M was observed to form fibrils much faster and to a greater extent than the WT protein, especially if we consider that a 3.5-fold higher concentration of the WT protein was used. When the changes in the light scattering leveled off (≈120 min for WT and 30 min for V30M), pressure was applied again to evaluate its effects on the fibril structure (Fig. 1*C*). In the case of WT fibrils, light scattering dropped immediately to a very low value, suggesting complete disassembly of the preformed WT fibrils and formation of a small, soluble species, likely the monomeric form.

The compression of V30M fibrils also leads to a large decrease in the light scattering; however, the final value was not as low as the one obtained for WT (Fig. 1*C*), suggesting incomplete/partial disassembly of V30M fibrils. There are at least two possibilities for interpreting the incomplete drop in the light scattering: (*i*) V30M fibrils are heterogeneous in terms of stability, and only the weaker fibrils are dissociated by HHP, thus forming a mixture of intact fibrils and small species; or (*ii*) V30M fibrils are homogeneous in terms of stability, and the whole population of fibrils is dissociated into an oligomeric species that scatters more light than the monomeric protein. In either case, the expected final value would be larger than the one displayed by monomers or tetramers of TTR.

The incomplete decrease in light scattering observed when V30M fibrils are compressed suggests that, if all of the population of V30M fibrils is equally sensitive to HHP (homogeneous in terms of stability), there is a core or a "stone" in the fibril of V30M that is pressure resistant. This observation may be physiologically relevant and have important implications regarding the stability of the fibrils against degradation and clearance strategies that could be adopted by the organism.

After 70 min under 3,000 bar, decompression gave rise to new fibrils in <30 min (Fig. 1*D*). Again, fibril formation by V30M occurred much faster and to a greater extent than the WT protein. Fig. 1 *E* and *F* shows that a third cycle of compression–decompression also induced the complete dissociation of WT fibrils but only a partial dissociation of V30M fibrils (Fig. 1*E*). V30M fibrils produced under acid conditions (incubation of 1 μM V30M at pH 5.0, 37°C, and at atmospheric pressure during 72 h) were also sensitive to HHP (data not shown).

These results indicate that TTR fibrils are sensitive to HHP, as are other amorphous aggregates and inclusion bodies (11, 12, 24). Because HHP is very effective in disrupting ionic and hydrophobic interactions but not in disrupting hydrogen bonds (reviewed in refs. 15 and 25), we can infer that the first two types of interactions have a major role in fibril maintenance. Because pressure shifts the equilibrium toward the species that occupies lower volume (15, 26), we can also conclude that there are packing defects in the fibrils that render them susceptible to dissociation by HHP. The results presented indicate that amyloid fibrils formed by the WT protein would be easier to clear than those formed by V30M, suggesting that the high propensity for amyloid fibril formation and the decreased clearance of V30M fibrils could contribute to the pathogenesis that leads to early-age onset in FAP. Recently, Sousa *et al.* (27) described preamyloidogenic forms of V30M in the nerves of early FAP patients. It is possible that the small oligomer we observed under pressure represents this initial prefibrillar conformation, which was also shown to be highly toxic to cell lines in culture (27).

To characterize the structure of the species released upon dissociation of the WT fibrils by HHP, we took advantage of the hydrophobic, fluorescent probe bis-ANS. The fluorescence intensity of bis-ANS emission (Fig. 1*G*) and its maximum emission wavelength (Fig. 1*H*) were used to monitor, respectively, the presence of binding sites for this probe and their relative hydrophobicity in the different species of TTR formed under consecutive cycles of compression–decompression. ANS and bis-ANS bind in the central channel (thyroxine-binding sites) of TTR and exhibit a red-shifted emission spectrum upon binding (28), consistent with the partial hydrophilic nature of this pocket (Fig. 1*H*, bar 1). Upon compression (+p), the fluorescence intensity of bis-ANS increases ≈5-fold in relation to the soluble protein, suggesting formation of a species with residual tertiary contacts able to bind bis-ANS (Fig. 1*G*, bar 2, and ref. 14). In addition, these new binding sites for bis-ANS are more hydrophobic and the maximum emission of the probe is located at 509 nm (Fig. 1*H*, bar 2). This result suggests that HHP is not denaturing TTR completely but instead converting it into a partially folded, monomeric conformation. In contrast, the fully unfolded state of TTR induced by urea does not bind bis-ANS (Fig. 1*G*, bar 6). When pressure is released and fibrillogenesis takes place, there is a further increase of 15% in bis-ANS emission and an added displacement in the maximum emission

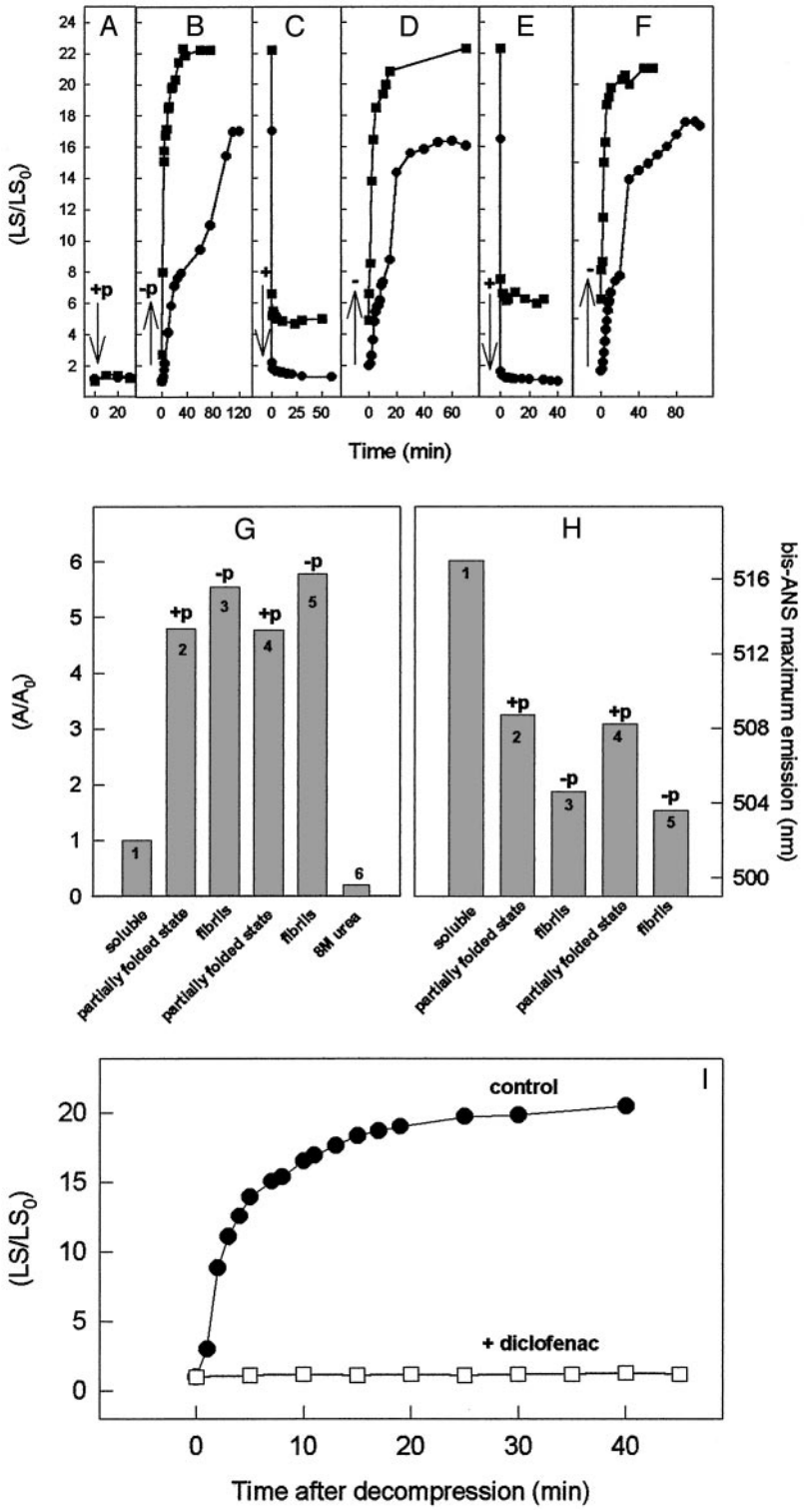

Fig. 1. (*A–F*) HHP induces dissociation of fibrils of WT and V30M TTR. (*A*) WT TTR (3.5 μM, ●) or V30M (1 μM, ■) was compressed at 3,000 bar (+p) at pH 5 and 37°C for 30 min. Then, pressure was released (−p), and the light scattering (LS) was recorded for 2 h (*B*). When the LS increase leveled off, pressure (+) was applied again (*C*). (*D–F*) Another round of decompression (−), compression (+), and decompression (−), respectively. LS was measured at 320 nm. (*G* and *H*) The species rescued from the WT fibrils is partially folded and binds bis-ANS. An experiment similar to that described in *A–F* was performed in the presence of bis-ANS (2 μM WT TTR and 20 μM bis-ANS) but measuring its fluorescence intensity (*G*, left ordinate) and maximum emission wavelength (*H*, right ordinate). Consecutive cycles of compression (+p)/decompression (−p) are shown, and the bars in *G* and *H* represent the following: 1, sample at atmospheric pressure (soluble, native tetramer); 2, sample after 60 min at 3,000 bar (partially folded state); 3, after returning to atmospheric pressure (fibril formation); 4 and 5, another cycle of compression (partially folded state) and decompression (fibril formation), respectively; and 6, the binding of bis-ANS to the urea-unfolded WT protein. (*G*) The binding of bis-ANS under different conditions is normalized to its binding to the native tetramer (A/A_0). (*I*) Diclofenac inhibits WT TTR fibrillogenesis. Wt TTR (3.5 μM) was compressed at 3,000 bar in absence of diclofenac at 37°C. After 60 min, the decompression was performed at 1°C to avoid aggregation. The high-pressure cuvette was opened on ice, and 70 μM diclofenac was added to the sample. Then, the temperature was raised to 37°C triggering aggregation, and the LS was recorded (□). A control curve (absence of diclofenac) is presented for comparison (●).

wavelength even more to the blue (Fig. 1*H*, bar 3), which is compatible with the existence in TTR fibrils of hydrophobic pockets accessible to the probe.

In the second cycle of compression, which results in complete dissociation of WT TTR fibrils (Fig. 1*C*), there is a small decrease in bis-ANS emission (Fig. 1*G*, bar 4), which returns to the same level seen in the first compression (Fig. 1*G*, bar 2). In addition, a red shift (from 504 to 509 nm) of the maximum emission (Fig. 1*H*, bar 4) to the previous position is observed. This result suggests that pressure induces recovery of a species with persistent tertiary contacts rather than the completely unfolded monomer or the native tetramer. Finally, when pressure is released, the fibrils are formed again and the bis-ANS emission returns to the higher value (Fig. 1*G*, bar 5) with a blue-shifted emission.

In addition to the changes in spectroscopic behavior of bis-ANS upon fibril formation and dissociation, the maximum emission wavelength of tryptophan (Trp) can furnish insight into the environment experienced by this residue during its lifetime.

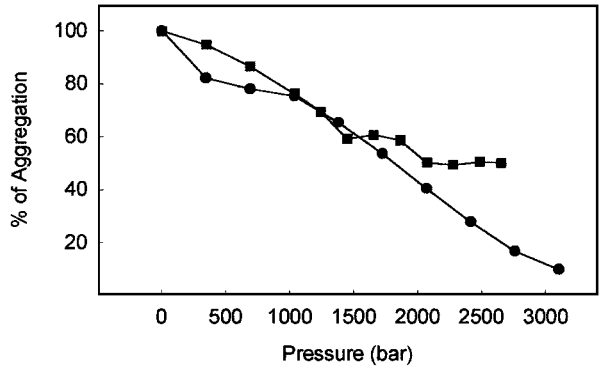

Fig. 2. Pressure titration of WT (●) and V30M (■) fibrils. The soluble proteins were subjected to a cycle of compression–decompression under aggregating conditions (pH 5, 37°C) to induce fibril formation. Then, pressure was applied in steps and the light scattering was recorded as in Fig. 1. The initial light scattering value of the fibrils was taken as 100% aggregation.

The Trp residues in the V30M and WT TTR tetramers face a similar environment, based on similar emission wavelengths (342–343 nm). Upon compression, a partially unfolded species accumulates and the Trp residues are exposed to the aqueous environment (maximum emission shifts to the red by ≈5–6 nm). When fibrillogenesis takes place after pressure release, the maximum emission is strongly blue-shifted (340–341 nm), which is compatible with Trp burial in the fibril core.

Recently, several nonsteroidal antiinflammatory drugs have been described to inhibit TTR fibrillogenesis by stabilizing the native tetrameric structure and preventing the formation of the monomeric amyloidogenic intermediate (29–31). We sought to investigate whether addition of diclofenac, a known inhibitor of TTR acid-induced amyloid fibril formation, could also be effective in preventing fibrillogenesis after an amyloidogenic conformation had been generated (Fig. 1*I*). Therefore, the drug was added after the first cycle of compression at 1°C (i.e., to the altered tetramer, T_4*) and then the temperature was raised up to 37°C to trigger amyloid fibril formation. Fig. 1*I* shows that diclofenac completely inhibits aggregation of WT TTR even when it has been primed to the amyloidogenic state (previous treatment with pressure). In conclusion, the species present after decompression (T_4*) not only binds bis-ANS more strongly than the native protein, but it also binds the ligand diclofenac, which blocks reaggregation. We propose that this cyclic high-pressure methodology would be useful for drug screening because after pressure release fibrillogenesis occurs very rapidly, requiring few minutes for completion what allows the screening of a large amount of compounds in a short period and in more amenable pH range (pH >5 instead of <4).

To better characterize the difference in stability between WT and V30M fibrils, high-pressure titration curves were performed (Fig. 2). Again, the WT fibrils were completely dismantled by HHP, whereas V30M fibrils were only partially dissociated (Fig. 2). It is worth emphasizing that the $p_{1/2}$ value (half-maximal dissociation) observed for WT TTR fibrils was 1,750 bar, a value that is close to those reported for the dissociation of dimers (for instance, Arc Repressor), trimers (allophycocyanin), tetramers (lactate dehydrogenase), and other oligomers (virus particles in general) (15, 26). In fact, the $p_{1/2}$ value found for the dissociation-denaturation of WT TTR tetramers at 37°C was equal to 2,700 bar (14), even larger than that reported here for the WT fibrils. This result suggests that the contacts that hold the protein tightly packed into the fibrils are weaker than those present among the monomers in the tetramer. Because of the greater sensitivity of TTR fibrils to HHP in comparison to the tetramer, we infer that van der Waals minima for the protein–protein contacts are less satisfied inside the fibrils than in the tetramer; this generates void

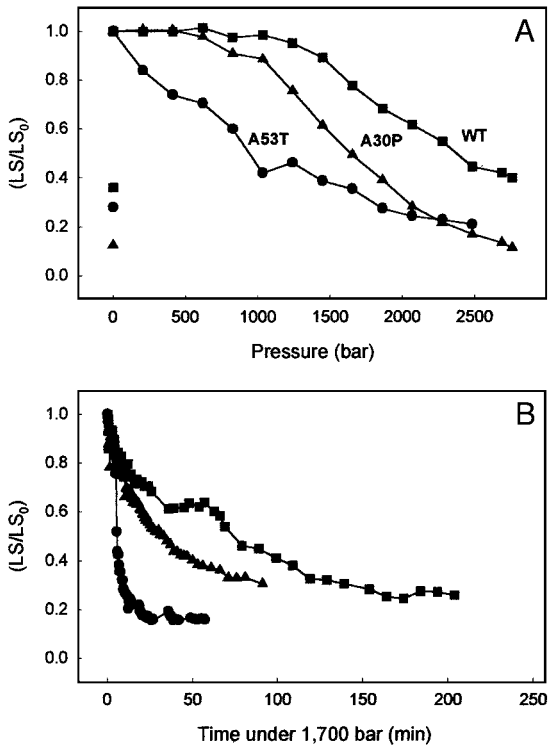

Fig. 3. (*A*) Pressure titration of α-syn fibrils from WT and variant proteins. Fibrils were produced at atmospheric pressure (see text) and then subjected to increasing pressure at 37°C while recording the light scattering (LS) as in Fig. 1. Proteins were: WT (■), A53T (●), and A30P (▲). The isolated symbols on the left represent the LS values obtained after decompression. (*B*) Kinetics of the pressure-induced dissociation of WT and variant fibrils of α-syn. The fibrils solutions were compressed at 1,700 bar at 37°C. The extent of fibril dissociation was recorded at intervals as a decrease in LS in comparison to the initial value (LS_0). Symbols are same as in *A*.

volumes inside the fibrils. Curiously, the $p_{1/2}$ values for the dissociation-denaturation of L55P and V30M tetramers were 1,500 and 1,850 bar, respectively (32); these values are much closer to that observed for the dissociation of WT TTR fibrils. This result suggests that the contacts that hold the WT TTR fibrils together are weak as those already present in the tetramers of the amyloidogenic variants of TTR, which may be related to the tendency for variants to undergo fibrillogenesis much faster and also to exhibit lower thermodynamic stability.

Pressure-Induced Dissociation of Preformed Fibrils of α-syn. Although ≈20 different proteins have been found to be involved in amyloidogenic diseases, most of them are unrelated structurally at the level of primary sequence. Despite these differences, all of the amyloid fibrils from different pathologies display common properties. Typically, they consist of two to six unbranched profilaments (2–5 nm wide) associated laterally or twisted together to form the fibrils that are 4–13 nm wide (33). The cross β-sheet topology has been observed in all fibrils thus far analyzed (34). To investigate how another type of amyloid fibril responds to HHP, we examined fibrils formed from α-syn, the amyloid protein involved in Parkinson's disease. Solutions of α-syn were incubated for 6 days (WT and A30P) or 24 h (A53T) at 37°C and pH 7.5 under gentle agitation to induce fibrillogenesis. At this time, in which the increase in *A* at 330 nm leveled off, the solutions of the WT and variant fibrils were subjected to increasing pressures (Fig. 3*A*), and the light scattering was measured at each pressure after 10 min equilibration. Scattering decreased as pressure was increased, indicating that α-syn fibrils are also sensitive to HHP (Fig. 3*A*). Interestingly, fibrils formed

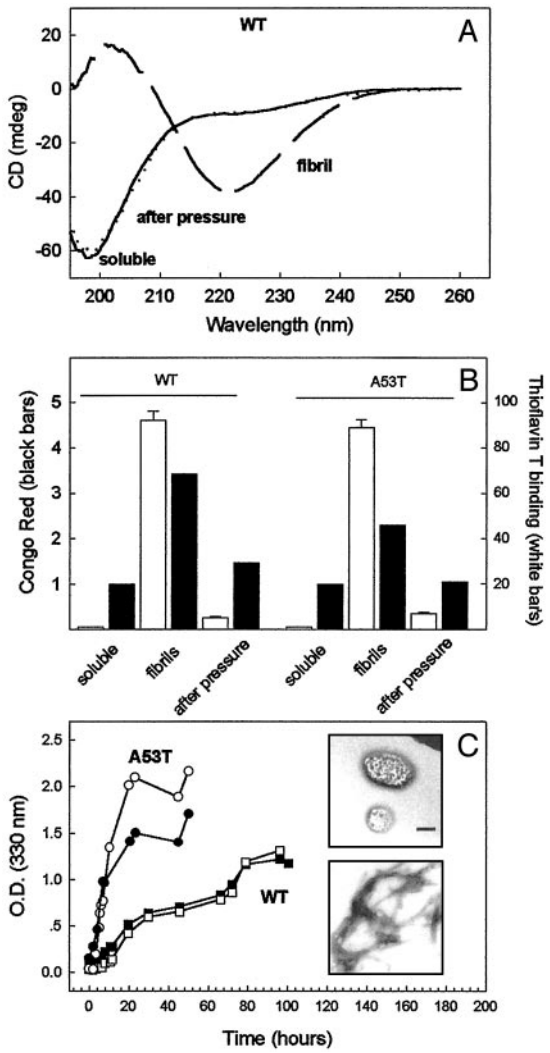

Fig. 4. Characterization of the species rescued from α-syn fibrils dissociated by HHP. (*A*) CD spectra of the soluble WT α-syn (continuous line); fibrils (long-dashed line); and the species rescued from HHP treatment (dashed line). (*B*) Binding of Congo red (filled bars) and thioflavin T (empty bars) to WT (*Left*) and A53T α-syn (*Right*) in the form of soluble protein, fibrils, and species rescued from the fibrils (after pressure). (*C*) Time course of fibril formation (see text) is expressed as the OD at 330 nm for the virgin, soluble protein (open symbols) and the soluble species rescued from the fibrils by HHP (filled symbols). Squares, WT protein; circles, A53T variant. (*Inset*) TEM images of the WT species rescued from the fibrils by HHP treatment (*Upper*) and of the fibrils reformed from this sample (*Lower*) after incubation under appropriate conditions (37°C, gentle agitation for 120 h). (Bar = 150 nm.)

from the PD-linked variants of α-syn were more sensitive to high pressure than the WT fibrils. The $p_{1/2}$ values were ≈800, 1,350, and 1,850 bar for the dissociation of A53T, A30P, and WT fibrils, respectively. After decompression of each protein, the light-scattering values remained low, showing no sign of aggregation (isolated symbols on the left in Fig. 3*A*). Taken together, these results suggest that HHP treatment converts the fibrils of α-syn into a soluble form that does not undergo fibrillogenesis immediately after pressure removal. The kinetics of fibril dissociation were examined at 1,700 bar (Fig. 3*B*). Again, the A53T fibrils dissociated more rapidly (<20 min) even at this moderate pressure, whereas the fibrils of A30P and WT protein dissociated much more slowly.

CD was used to obtain insight into the secondary structural changes induced by HHP treatment on the α-syn fibril structure. Fig. 4*A* shows the CD spectra of the WT soluble protein before

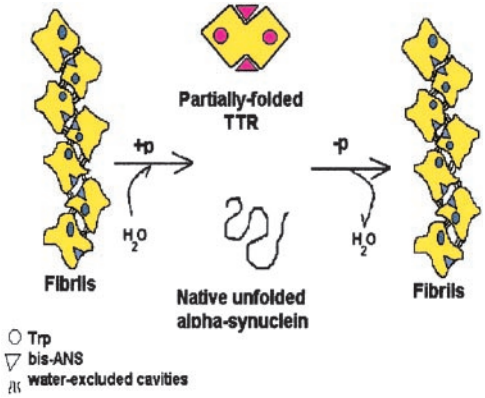

Fig. 5. Schematic representation of the effects of HHP on the fibrils of WT TTR and α-syn. The core of the amyloid fibrils is not perfectly packed, creating cavities that render the fibrils susceptible to HHP. Upon compression (+p), water infiltrates and dissociation takes place, forming either a partially folded species, as in the case of WT TTR, or a native, unfolded monomer, as in the case of α-syn. In the case of TTR fibrils, Trp and bis-ANS present a blue-shifted emission, suggesting that both fluorophores lie in nonpolar environments. Upon fibril dissociation, the partially folded species of TTR is formed, the Trps are exposed to solvent (red-shifted emission), and the bis-ANS binding pocket is more hydrophilic than in the fibrils. Upon pressure release (−p), the partially folded species of TTR reforms fibrils in <1 h, whereas the native, unfolded α-syn has lost none of its amyloidogenic properties and can aggregate as fast as the virgin, soluble protein.

fibrillogenesis and the spectra of the fibrils and of the species rescued from the fibrils after HHP. Before compression, soluble α-syn exhibited a CD signal (an ellipticity minimum at 198 nm) that is consistent with a predominantly random coil, whereas aggregated α-syn exhibited a signal (minimum at 220 nm) that is characteristic of a β-sheet-rich structure. The α-syn recovered from pressure denaturation of the fibrils revealed CD spectrum that is identical to the soluble protein, indicating that high pressure results in both dissociation and unfolding of α-syn fibrils (Fig. 4*A*).

To confirm the dissociation of α-syn fibrils by HHP, we used the amyloid specific dyes Congo red and thioflavin T to monitor the formation and dissociation of the α-syn fibrils as a function of pressure (Fig. 4*B*). Both WT and A53T fibrils bound the Congo red and thioflavin T consistent with the formation of a fibril-like structure. In contrast, the binding of both dyes to the species present after decompression was reduced to the same level as that observed for the soluble forms of the proteins.

To evaluate whether the species recovered from the fibrils by HHP treatment retains its ability to undergo self-assembly into amyloid fibrils, the samples were incubated after decompression under gentle agitation at 37°C and the aggregation was monitored by turbidity at 330 nm (Fig. 4*C*). The A53T variant undergoes aggregation faster than the WT protein, consistent with previous reports (17, 35). Interestingly, in both cases the aggregation time course observed for the soluble species rescued by pressure treatment was very similar to that seen for the soluble, virgin proteins. To investigate the presence or absence of fibrils in these samples, TEM images were collected (Fig. 4*C Inset*). Fig. 4*C Upper* shows that after decompression there are no detectable fibrils in the sample (although the fibrils were there before compression as seen by TEM, not shown). After incubating this sample under suitable conditions (gentle agitation at 37°C for 120 h), fibrils reappear showing a native-like morphology (Fig. 4*C Lower*). This result indicates that HHP treatment dissociates preformed fibrils of both WT and variant α-syn into soluble, native-like, and fibril-competent species, suggesting that α-syn fibrillogenesis is a reversible process under appropriate conditions.

Discussion

Our data show the high sensitivity of the amyloid fibers formed from α- syn and TTR to a physical agent such as HHP. The amyloid fibrils undergo dissociation in a pressure range comparable to that observed for small oligomers (26). Although the proteins composing the fibrils are well structured, they appear to have water-excluded cavities that make them highly susceptible to pressure denaturation (Fig. 5). The individual structure and stability of proteins and multimolecular assemblies reside in their packing characteristics (15, 36). Recent theoretical approaches provide a link between the hydration of hydrophobic surfaces and excluded volume (37, 38). Hydration can account for pressure effects such as those reported here: pressure causes infiltration of water molecules into the hydrophobic core of the protein. It has been previously shown that pressure denaturation does not occur when water is withdrawn (15, 39, 40). Pressure dissociates amyloid fibers because they possess water-excluded cavities that bind hydrophobic compounds such as bis-ANS. Fig. 5 depicts the findings described here. The main difference in behavior between TTR and α-syn is that the structured intermediate of TTR leads to fast reaggregation after decompression whereas the unstructured, soluble α-syn has a slow kinetics of aggregation equal to the native protein. These findings not only point toward possible mechanisms of pathogenesis but also imply that different strategies should be sought to attack the two diseases: for α-syn, compounds that destabilize any structured oligomer will be the best choice, whereas for TTR, only drugs that prevent the fibril formation may be effective. Above all, the water-excluded cavities that prevail in both types of fibrils (Fig. 5) should be considered in any search for the development of new drugs.

Our data also show that the pressure dissociation of fibrils occurs in the same time frame and in the same pressure range of that required for dissociation of native oligomeric proteins. This finding implies that the same properties allowing subunit dissociation of oligomeric proteins, such as packing defects and hydrophobic pockets, are likely present in the fibrils. Recently, Torrent *et al.* (41) described that high pressure (2,000 bar) dissociates the high temperature-induced aggregates of recombinant prion protein. However much higher pressures (12,000 bar) at high temperature conditions (>100°C) were recently demonstrated to be able to inactivate prion infectivity in processed meat (42). On the other hand, the yeast prion protein Ure2 undergoes only limited perturbation at a pressure of 6,000 bar (43).

Our data point to the use of HHP as a valuable tool for populating important intermediate states competent for fibrillogenesis, as demonstrated for TTR, as well as for the original native-unfolded species of α-syn. In the case of α-syn fibrils, the aggressive variants are more susceptible to pressure than WT. This result is significant in the light of recent evidence that oligomeric aggregates, rather than the fibrils themselves, are more important for the pathogenesis (44–46). In this respect, the weaker fibrils of the variants of α-syn would generate small oligomers when the cellular machinery tries to get rid of them. Whereas the mutant α-syn fibrils present easier dissociation than the WT form, a different pattern is found for the V30M TTR in comparison to WT TTR. In the case of TTR, the formation of pressure-resistant core derived from the V30M fibrils would also be more toxic and pathogenic than the soluble species derived from the WT fibrils.

In conclusion, our data show that the amyloid fibrils, although similar in architecture, present differences in stability probably related to the existence of packing defects in their core. These packing defects are generated by the imperfect contact between the side chains inside fibril structure, which suggests that the amino acid sequence may play an important role in fibril stability.

We are grateful to Emerson R. Gonçalves for competent technical assistance and Martha M. Sorenson for helpful comments on the manuscript. This work was supported in part by grants from Conselho Nacional de Desenvolvimento Científico e Tecnológico, Programa de Núcleos de Excelência, Fundação de Amparo à Pesquisa no Estado do Rio de Janeiro of Brazil (to D.F. and J.L.S.), a grant from the International Center for Genetic Engineering and Biotechnology (Italy) (to J.L.S.), and U.S. Public Health Service Grants from the National Institutes of Health (to J.W.K.). M.C.S. has a postdoctoral fellowship from Fundação Carlos Chagas Filho de Amparo à Pesquisa do Estado do Rio de Janeiro.

1. Sacchettini, J. C. & Kelly, J. W. (2002) *Nat. Rev. Drug Discov.* **4,** 267–275.
2. Holden, C. (2002) *Science* **297,** 500–502.
3. Coelho, T. (1996) *Curr. Opin. Neurol.* **9,** 355–359.
4. Horwich, A. (2002) *J. Clin. Invest.* **110,** 1221–1232.
5. Hammarstrom, P., Schneider, F. & Kelly, J. W. (2001) *Science* **28,** 2459–2462.
6. Spillantini, M. G., Schmidt, M. L., Lee, V. M. Y., Trojanowski, J. Q., Jakes, R. & Goedert, M. (1997) *Nature* **388,** 839–840.
7. Forno, L. S. (1996) *J. Neuropathol. Exp. Neurol.* **55,** 259–272.
8. Spillantini, M. G., Crowther, R. A., Jakes, R., Hasegawa, M. & Goedert, M. (1998) *Proc. Natl. Acad. Sci. USA* **95,** 6469–6473.
9. Polymeropoulos, M. H., Lavedan, C., Leroy, E., Ide, S. E., Dehejia, A., Dutra, A., Pike, B., Root, H., Rubenstein, J., Boyer, R., *et al.* (1997) *Science* **276,** 2045–2047.
10. Benson, M. D. (1989) *Trends Neurosci.* **12,** 88–92.
11. Gorovits, B. M. & Horowitz, P. M. (1998) *Biochemistry* **37,** 6132–6135.
12. Foguel, D., Robinson, C. R., deSousa, P. C., Jr., Silva, J. L. & Robinson, A. S. (1999) *Biotechnol. Bioeng.* **63,** 552–558.
13. Meersman, F., Smeller, L. & Heremans, K. (2002) *Biophys. J.* **82,** 2635–2644.
14. Ferrão-Gonzales, A. D., Souto, S. O., Silva, J. L. & Foguel, D. (2000) *Proc. Natl. Acad. Sci. USA* **97,** 6445–6450.
15. Silva, J. L., Foguel, D. & Royer, C. A. (2001) *Trends Biochem. Sci.* **26,** 612–618.
16. Lai, Z., Colon, W. & Kelly, J. W. (1996) *Biochemistry* **35,** 6470–6482.
17. Conway, K. A., Harper, J. D. & Lansbury, P. T., Jr. (1998) *Nat. Med.* **4,** 1318–1320.
18. Glover, J. R., Kowal, A. S., Schirmen, E. C., Patino, M. M., Liu, J. & Lindquist, S. (1997) *Cell* **89,** 811–819.
19. MacCutchen, S. L., Kelly, J. W. & Colon, W. (1993) *Biochemistry* **32,** 12119–12127.
20. MacCutchen, S. L., Lai, Z., Miroy, G., Kelly, J. W. & Colon, W. (1995) *Biochemistry* **34,** 13527–13536.
21. Lashuel, H. A., Lai, Z. & Kelly, J. W. (1998) *Biochemistry* **37,** 17851–17864.
22. Quintas, A., Saraiva, M. J. & Brito, R. M. M. (1999) *J. Biol. Chem.* **274,** 32943–32949.
23. Hammarstrom, P., Jiang, X., Hurshman, A. R., Powers, E. T. & Kelly, J. W. (2002) *Proc. Natl. Acad. Sci. USA* **99**, 16427–16432.
24. St. John, R. J., Carpenter, J. F. & Randolph, T. W. (1999) *Proc. Natl. Acad. Sci. USA* **96,** 13029–13033.
25. Heremans, K. & Smeller, S. (1998) *Biochim. Biophys. Acta* **2,** 353–370.
26. Silva, J. L. & Weber, G. (1993) *Annu. Rev. Phys. Chem.* **44,** 89–113.
27. Sousa, M. M., Cardoso, I., Fernandes, R., Guimaraes, A. & Saraiva, M. J. (2001) *Am. J. Pathol.* **6,** 1993–2000.
28. Rosen, H. N., Moses, A. C., Murell, J., Liepnieks, J. J. & Benson, M. D. (1993) *J. Clin. Endocrinol. Metab.* **77,** 370–374.
29. Baures, P. W., Oza, V. B., Peterson, S. A. & Kelly, J. W. (1999) *Bioorg. Med. Chem.* **7,** 1339–1347.
30. Klabunde, T., Petrassi, H. M., Oza, V. B., Raman, P., Kelly, J. W. & Sacchettini, J. C. (2000) *Nat. Struct. Biol.* **4,** 312–321.
31. Oza, V. B., Smith, C., Raman, P., Koepf, E. K., Lashuel, H. A., Petrassi, H. M., Chiang, K. P., Powers, E. T., Sachettinni, J. & Kelly, J. W. (2002) *J. Med. Chem.* **45,** 321–332.
32. Ferrão-Gonzales, A. D., Palmieri, L. C., Valory, M., Silva, J. L., Lashuel, H., Kelly, J. W. & Foguel, D. (2003) *J. Mol. Biol.* **328,** 963–974.
33. Serpell, L. C., Sunde, M., Benson, M. D., Tennent, G. A., Pepys, M. B. & Fraser, P. A. (2000) *J. Mol. Biol.* **300,** 1033–1039.
34. Wood, S. J., Wypych, J., Steavenson, S., Louis, J. C., Citron, M. & Biere, A. L. (1999) *J. Biol. Chem.* **274,** 19509–19512.
35. Li, J., Uversky, V. N. & Fink, A. L. (2001) *Biochemistry* **40,** 11604–11613.
36. Eriksson, A. E., Baase, W. A., Zhang, X. J., Heinz, D. W., Blaber, M., Baldwin, E. P. & Matthews, B. W. (1992) *Science* **255,** 178–183.
37. Hummer, G., Garde, S., Garcia, A. E., Paulaitis, M. E. & Pratt, L. R. (1998) *Proc. Natl. Acad. Sci. USA* **95,** 1552–1555.
38. Hillson, N., Onuchic, J. N. & Garcia, A. E. (1999) *Proc. Natl. Acad. Sci. USA* **96,** 14848–14853.
39. Oliveira, A. C., Gaspar, L. P., Da Poian, A. T. & Silva, J. L. (1994) *J. Mol. Biol.* **240,** 184–187.
40. Foguel, D. & Silva, J. L. (1994) *Proc. Natl. Acad. Sci. USA* **17,** 8244–8247.
41. Torrent, J., Alvarez-Martinez, M. T., Heitz, F., Liautard, J. P., Balny, C. & Lange, R. (2003) *Biochemistry* **42,** 1318–1325.
42. Brown, P., Meyer, R., Cardone, F. & Pocchiari, M. (2003) *Proc. Natl. Acad. Sci. USA* **100,** 6093–6097.
43. Zhou, J.-M., Zhu, L., Balny, C. & Perrett, S. (2001) *Biochem. Biophys. Res. Commun.* **287,** 147–152.
44. Goldberg, M. S. & Lansbury, P. T., Jr. (2000) *Nat. Cell Biol.* **7,** E115–E119.
45. Bucciantini, M., Giannoni, E., Chiti, F., Baroni, F., Formigli, L., Zurdo, J., Taddei, N., Ramponi, G., Dobson, C. M. & Stefani, M. (2002) *Nature* **416,** 507–511.
46. Lashuel, H. A., Hartley, D., Petre, B. M., Walz, T. & Lansbury, P. T., Jr. (2002) *Nature* **418,** 291.